The Cell Surface 13 (2025) 100136

Contents lists available at ScienceDirect

The Cell Surface

journal homepage: www.sciencedirect.com/journal/the-cell-surface

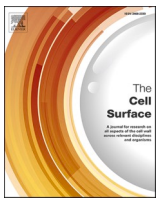

Spatiotemporal regulation of alginate sub-structures at multiple scales revealed by monoclonal antibodies

Catherine T. Jones [a,b,1], Cassie Bakshani [a,c,1], Ieva Lelenaite [a], Jozef Mravec [d,e], Stjepan Krešimir Kračun [d,f], Jeff Pearson [g], Mathew D. Wilcox [g], Kevin Hardouin [h], Sonia Kridi [h], Cécile Hervé [h], William G.T. Willats [a,*]

[a] School of Natural and Environmental Sciences, Newcastle University, Newcastle Upon Tyne NE1 7RU, UK
[b] Current Affiliation: Leica Biosystems Newcastle Ltd, Balliol Business Park, Benton Lane, Newcastle Upon Tyne NE12 8EW, UK
[c] Current Affiliation: Institute of Microbiology and Infection, College of Medical and Dental Sciences, University of Birmingham, Birmingham, B15 2TT, UK
[d] Department of Plant and Environmental Sciences, University of Copenhagen, Thorvaldsensvej 40, 1871, Denmark
[e] Current Affiliation: Institute of Plant Genetics and Biotechnology, Plant Science and Biodiversity Centre, Slovak Academy of Sciences, Akademická 2, 94901 Nitra, Slovakia
[f] Current Affiliation: Novonesis A/S, Gammel Venlighedsvej, 142970 Hørsholm, Denmark.
[g] Newcastle University Biosciences Institute, The Medical School, University of Newcastle Upon Tyne Framlington Place, Newcastle upon Tyne NE2 4HH, UK
[h] CNRS / Sorbonne Université, Station Biologique De Roscoff, Place Georges Teissier, 29680 Roscoff, France

ARTICLE INFO

Keywords:
Alginate
Monoclonal antibodies
Algae
Algal cell walls
NMR

ABSTRACT

Alginates are abundant linear polysaccharides produced by brown algae and some bacteria. They have multiple biological roles and important medical and commercial uses. Alginates are comprised of D-mannuronic acid (M) and L-guluronic acid (G) and the ratios and distribution patterns of M and G profoundly impact their physiological and rheological properties. The structure/function relationships of alginates have been extensively studied in vitro but our understanding of the in vivo spatiotemporal regulation of alginate fine structures and their biological implications is limited. Monoclonal antibodies (mAbs) are powerful tools for localising and quantifying glycan structures and several alginate-directed mAbs have been developed. We used a library of well-defined alginates, with M and G block ratios determined by NMR, to refine our understanding of the binding properties of alginate-directed mAbs. Using these probes, we obtained new insight into how structural features of alginates are regulated at different scales, from cellular to seasonal.

1. Introduction

Alginates are unbranched biopolymers produced as cell wall components by brown algae and as exopolysaccharides by some bacteria including *Azotobacter vinelandii*, *A. chroococcum* and several species of *Pseudomonas* (Mazéas et al., 2023; Thomas et al., 2016). Alginates are comprised of 1,4-linked β-D-mannuronic acid (M) and α-L-guluronic acid (G). These residues may be linked in a variety of sequential structures including homopolymeric regions of M and G blocks interspaced with regions of alternating M and G blocks (Ertesvåg, 2015; Mazéas et al., 2023; Thomas et al., 2013; Thomas et al., 2016).

In brown algae, alginate is initially synthesised as mannuronan which may be subsequently modified by mannuronan C5-epimerases (ManC5-Es) which catalyse the conversion of M residues into G residues (Ertesvåg, 2015; Mazéas et al., 2023). This post-synthetic processing yields alginates with varying M and G compositions and distributions, and hence differences in their rheological characteristic, for example gelling properties and plasticity (Skjåk-Bræk et al., 2015). The structure/function relationships of alginates have been extensively studied in the context of their multiple industrial and medical applications, but the biological significance and regulation of their fine structures is less well understood. In part, this is because most analytical techniques for determining M and G composition and distribution are performed on extracted samples so that much of the biological context is lost.

Molecular probes including monoclonal antibodies (mAbs) and

* Corresponding author.
E-mail address: William.Willats@newcastle.ac.uk (W.G.T. Willats).
[1] Joint first authors

https://doi.org/10.1016/j.tcsw.2024.100136
Received 22 October 2024; Received in revised form 26 November 2024; Accepted 5 December 2024
Available online 8 December 2024

carbohydrate binding modules (CBMs) have been used extensively to study structure/function relationships and cellular localisations of land plant polysaccharides (Fangel et al., 2024; Knox, 2008; Lee et al., 2011; Rydahl et al., 2018). To a lesser extent, these probes have also been used to study algal and bacterial cell walls and exopolysaccharides. In the case of alginate, several mAbs (the 'BAM' series) have been described that bind to epitopes with differing M and G configurations (Thomas et al., 2016). These mAbs have extended our understanding of cell wall biology in brown algae, for example, the dynamics of cell wall assembly during early embryogenesis in *Fucus* sp. (Mazéas et al., 2023). In addition, some commercial anti-alginate antibodies are available, although the epitopes recognised by them are not well defined.

In this work, we used a library of well-defined alginates, with M and G block ratios determined by nuclear magnetic resonance (NMR), to refine our understanding of the binding properties of alginate-directed mAbs. With this information, we then used the mAbs to explore the regulation of epitopes with different M and G structures at different scales, at the cellular level in single species to seasonal variations across multiple species.

2. Materials and methods

2.1. Mapping specificities of alginate-directed mAbs using microarrays

The specificities of mAbs were determined by assessing their binding to alginate samples printed as microarrays. A library of 32 alginates was assembled consisting of samples with varying M and G blocks ratios determined previously by NMR (**Supplemental Table 1**) (Chater et al., 2015). Alginates were obtained from FMC BioPolymer (Haugesund, Norway) and the method used to determine the M and G ratios was as described (Bojorges et al., 2023)). Samples were dissolved in water to a concentration of 5 mg/mL then a further three serial 5-fold-dilutions were prepared. Samples were mixed 1:1 with array printing buffer (0.8 % Triton X-100, 55.2 % glycerol, 44 % water) to give a final concentration range of 0.02 mg/mL - 2.5 mg/mL. Samples were printed in triplicate as microarrays onto nitrocellulose using a non-contact microarray robot (ArrayJet, Roslin, Scotland) as described previously (Bakshani et al., 2023; Fangel et al., 2024).

Microarrays were probed with monoclonal antibodies, with binding detected using anti-rat, anti-mouse or anti-His-tag secondary antibodies, as appropriate, and conjugated to alkaline phosphatase (Bakshani et al., 2023 and Fangel et al., 2024). The mAbs used are detailed in **Supplemental Table 2**. Microarray outputs were processed using microarray analysis software (Array-Pro Analyzer, v.6.3.1, Media Cybernetics, Rockville, USA) and mean spot signals from dilutions and three replicates were calculated as described previously (Bakshani et al., 2023 and Fangel et al., 2024). The highest mean spot signal in the data set was adjusted to 100 and all other mean spot signals were normalised accordingly.

2.2. Immunofluorescence localisation of alginate epitopes

Fucus vesiculosus was collected in the Øresund on the Baltic coast and thalli were cut into small pieces of approximately 5 mm × 5 mm. Samples were washed with phosphate-buffer saline (PBS) and fixed in 1 mL 4 % paraformaldehyde in PBS under vacuum for 20 min in a desiccator chamber connected to a vacuum pump. Fixative was removed and the samples washed twice with 1 mL PBS. Dehydration was performed using an ethanol dilution series with PBS (30 %, 50 %, 70 %, 96 %, and absolute ethanol) using 1 mL of each with 10 min incubation time. Absolute ethanol was removed, and a mix of LR white (Agar Scientific, London, UK) with absolute ethanol 1:1 was added for 3 h then replaced with pure LR White and left overnight. Gelatine capsules were filled with LR White, and the sample pieces were added and oriented. Polymerization was performed at 60 °C for 24 h. The gelatine was wetted with water and removed. The blocks were sectioned with an ultramicrotome (Leica UC7) and a glass knife to produce 1 μm sections, which were adhered in water drops at 60 °C to charged SuperFrost slides (Thermo Fisher). Enzymatic treatments were done directly on the sections using *Sphingomonas* sp. alginate lyase (Megazyme, Bray, Ireland) at 2.5 U/mL in PBS for 1 h at room temperature and washed twice with PBS before probing.

The area around the adhered sections was marked with PAP PEN (Agar Scientific, London, UK) and left to dry. The sections were blocked with 5 % (weight/volume) milk powder in PBS (MP/PBS) for 30 min, then primary antibody in MP/PBS was added for 1 h at room temperature. After washing three times with PBS, secondary antibody in MP/PBS at 1:300 dilution was added and incubated 1 h at room temperature and washed 3 times with PBS. Finally, Calcofluor White was added at a 1:100 dilution in PBS for 5 min and then washed with PBS. Samples were mounted in Citifluor (Agar Scientific, London. UK) and observed immediately. The commercial antibodies 4BIO 1C5 (Invitrogen) and 3G4-1F3 (Sigma) were used at 1:100 dilution and BAM series antibodies were used at 1:10 dilution. Anti-rat or mouse anti-IgG secondary antibody conjugated to AlexaFluor 555 and AlexaFluor 488 respectively (Thermofisher) were applied at a 1:300 dilution. Laser scanning confocal microscopy was performed using an inverted microscope (Leica SP5) equipped with a 405 nm UV diode (for Calcofluor white), and an argon 488 nm laser was used for AlexaFluor 488 and GFP and HeNe (543 nm) for AlexaFluor 555. Images were processed in LAS X (Leica) and GIMP II software.

2.3. Analysis of alginate epitopes in wild algal species

17 wild growing algae were collected from the Brittany coast near Roscoff, France (coordinates 48°43′49"N 3°59′36"W) on four different occasions (October 2015, April 2016, October 2016 and April 2017) (**Supplemental Table 3**). Nine species were from the Fucales order (*Ascophyllum nodosum*, *Bifurcaria bifurcata*, *Fucus serratus*, *Fucus spiralis*, *Fucus vesiculosus*, *Halidrys siliquosa*, *Himanthalia elongata*, *Sargassum muticum, Pelvetia Canaliculata*), one from the Tilopteridales order (*Saccorhiza polyschides*), four from the Laminariales order (*Laminaria digitata*, *Laminaria hyperborea*, *Saccharina latissima*, *Undaria pinnatifida*), two from the Dictyotales order (*Dictyopteris polypodioides*, *Dictyota dichotoma*) and two from the Ectocarpales order (*Colpomenia peregrina*, *Pylaiella littoralis*). All samples were dried in a ventilated oven at 50 °C for at least 24 h and finely ground using an oscillating ball mill (FastPrep® System, MP Biomedicals©, USA) at a speed of 6.5 ms^{-1} for 30 s.

Alcohol-insoluble residues (AIRs) were prepared using an automated solvent extractor (ASE™, Thermo Scientific™, Dionex). The ground algae (300 mg) were first extracted with 80 % ethanol, at a flow rate of 2 mL/min, at 100 °C for 12 min, followed by an 80 % ethanol/20 % acetone treatment in the same conditions for 18 min. Cell-wall polymers were sequentially extracted from AIR using a dedicated protocol for brown algae and based on the sequential use of 2 % $CaCl_2$ for 2 h at 70 °C, pH 2 HCl for 2 h at 70 °C, 3 % Na_2CO_3 for 2 h at 80 °C and 4 M KOH for 2 h at room temperature. Samples were centrifuged between each extraction (3000 xg, 10 min) and the supernatants collected.

3. Results

3.1. Binding specificities of molecular probes

7 alginate-directed mAbs (detailed in **Supplemental Table 2**) were screened for binding against 32 well-defined alginate samples (PAA-RB12, detailed in **Supplemental Table 1**), two commercial alginates and three pectins. Three anti-homogalacturonan mAbs (LM7, LM18 and JIM5) were also tested. Mean binding intensities (from three independent experiments) are presented as a heatmap in Supplemental Fig. 1.

The well-defined alginate samples had previously been analysed using NMR to determine their M and G block structures in terms of the fractions of total M residues, total G residues, GG homodimers, GGG

homotrimers, MGM heterotrimers, MGG heterodimers and FF homodimers (Chater et al., 2015). For example, sample PAA has a F(M) value of 0.2, an F(G) value of 0.8, an F(MM) value of 0.1 and a F(GG) value of 0.7 – meaning that in this samples 20 % of the residues are M (50 % of which exist as MM homodimers) and 80 % of the residues are G (of which 87.5 % exist as GG homodimers).

The microarray data indicated that mAbs BAM6–10 had broadly similar binding profiles across the alginate sample set with notably weaker binding to samples PAB, PAV, PAW, PAX and PAY. The two commercial mAbs (4B10—1C5 and 3G4-1F3) exhibited similar binding profiles and avidities to each other, but distinct to the BAM mAbs, with more promiscuous binding across the alginate sample set, but with notably weaker binding to sample PAG (Supplemental Fig. 1).

It has previously been reported that BAM7 cross-reacts to homogalacturonan (HG) (Thomas et al., 2016). We confirmed this because BAM7 (but no other BAM mAbs) bound to the three pectin samples included on the microarray (Supplemental Fig. 1**)**. Conversely, we also found that LM7, a mAb that has previously been characterised as binding to HG (Willats et al., 2001), also cross-reacts with alginates with a binding profile similar to that of BAM7, BAM8 and BAM9 (Supplemental Fig. 1**)**. LM7 bound only weakly to the pectin samples on the microarray, and this may be due to the precise binding requirements of LM7 with regard to the extent and distribution of methyl esters on HG not being present on these particular samples.

To help decipher the complex relationships between probe binding and alginate M and G content and distribution, we determined Pearson correlation coefficients (PCCs) for mAb binding versus G and M content and distribution of all the well-defined alginate samples. PCC data are presented as a heatmap in Supplemental Fig. 2**.** Strong positive and negative correlations between mAb binding and particular M and G block ratios are shown as green and red, respectively, in the heatmap. The PCC data heatmap revealed that the mAb binding profiles broadly fell into four groups: 1) BAM7, BAM8, BAM9 and LM7; 2) BAM6; 3) BAM10 and 4) 4BIO-1C5 and 3G4-1F3.

To simplify interpretation, PCC data for one representative mAb from each group are also presented as bar graphs in Fig. 1. BAM6 binding was positively correlated with M and MM but negatively correlated with G, GM and MGM (Fig. 1A). Conversely, BAM10 binding was positively correlated with G, GG and GGG but negatively correlated with M, GM and MGM (Fig. 1B). BAM7 (also representative of BAM8, BAM9 and LM7) binding was positively correlated with both GG, GGG and MM, but negatively correlated with GM and MGM (Fig. 1C). Finally, 4BIO-1C5 (also representative of 3G4-1F3) binding was positively correlated with G, GG, and GGG but negatively correlated with GM, MGM, M and MM (Fig. 1D).

3.2. *Immunofluorescence localisation of alginate epitopes*

Immunofluorescence microscopy was used to determine the cellular locations of alginate epitopes. mAbs were applied to thin sections through *Fucus vesiculosus* receptacles (Fig. 2). In some case, sections were pretreated with alginate lyase from *Sphingomonas* sp. prior to probing (Figs. 2F-2J and 2N-2P). Low magnification toluidine blue sections showing receptacle anatomy are shown in Supplemental Fig. 3, with the position of the immunofluorescence labelling shown in Figs. 2 and 3 indicated.

Reflecting the PCC data, BAM6, BAM8 and BAM9 exhibited similar localisation patterns, with labelling most intense in the septum of tissue between concepticles and sparser labelling within concepticles themselves (Figs. 2A-2C). BAM7 and BAM10 binding was generally weaker

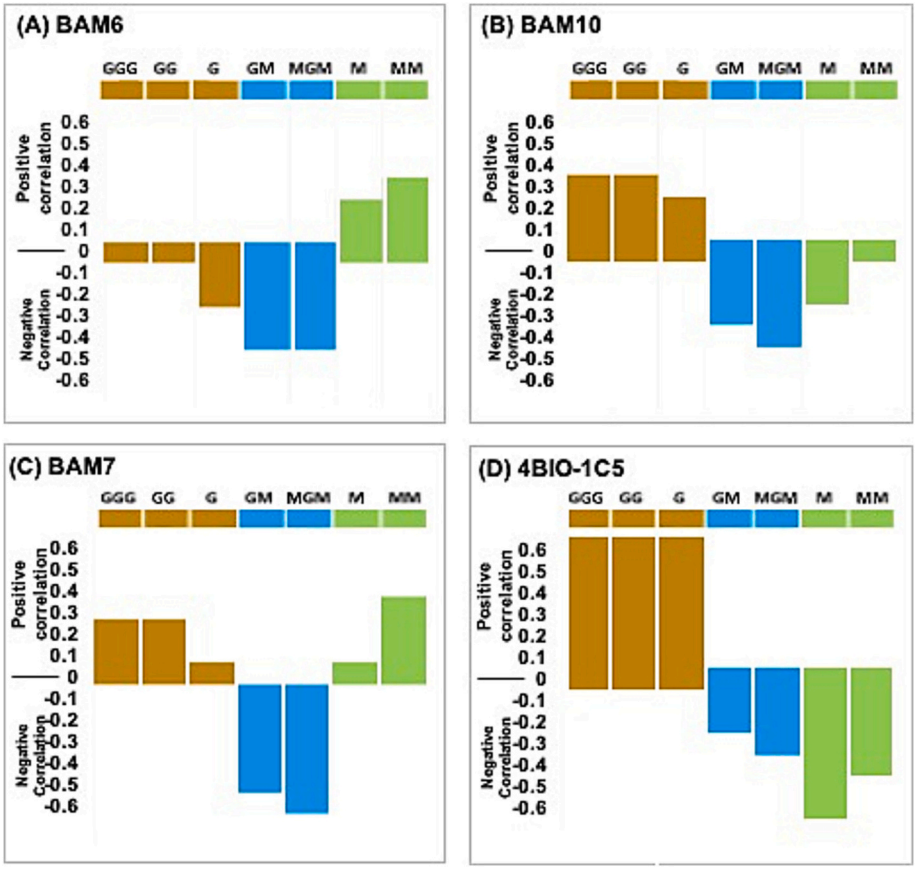

Fig. 1. Bar graphs showing pearson correlation coefficients (PCCs) for BAM6 (A), BAM10 (B), BAM7 (C) and 4BIO-1C5 (D) to alginate samples (as determined using microarrays). The values show the strength of linear association between antibody binding signals and the content and distribution of guluronate (G) and mannuronate (M) residues in the alginates. Values closer to +1 and − 1 indicate stronger positive and negative correlations, respectively.

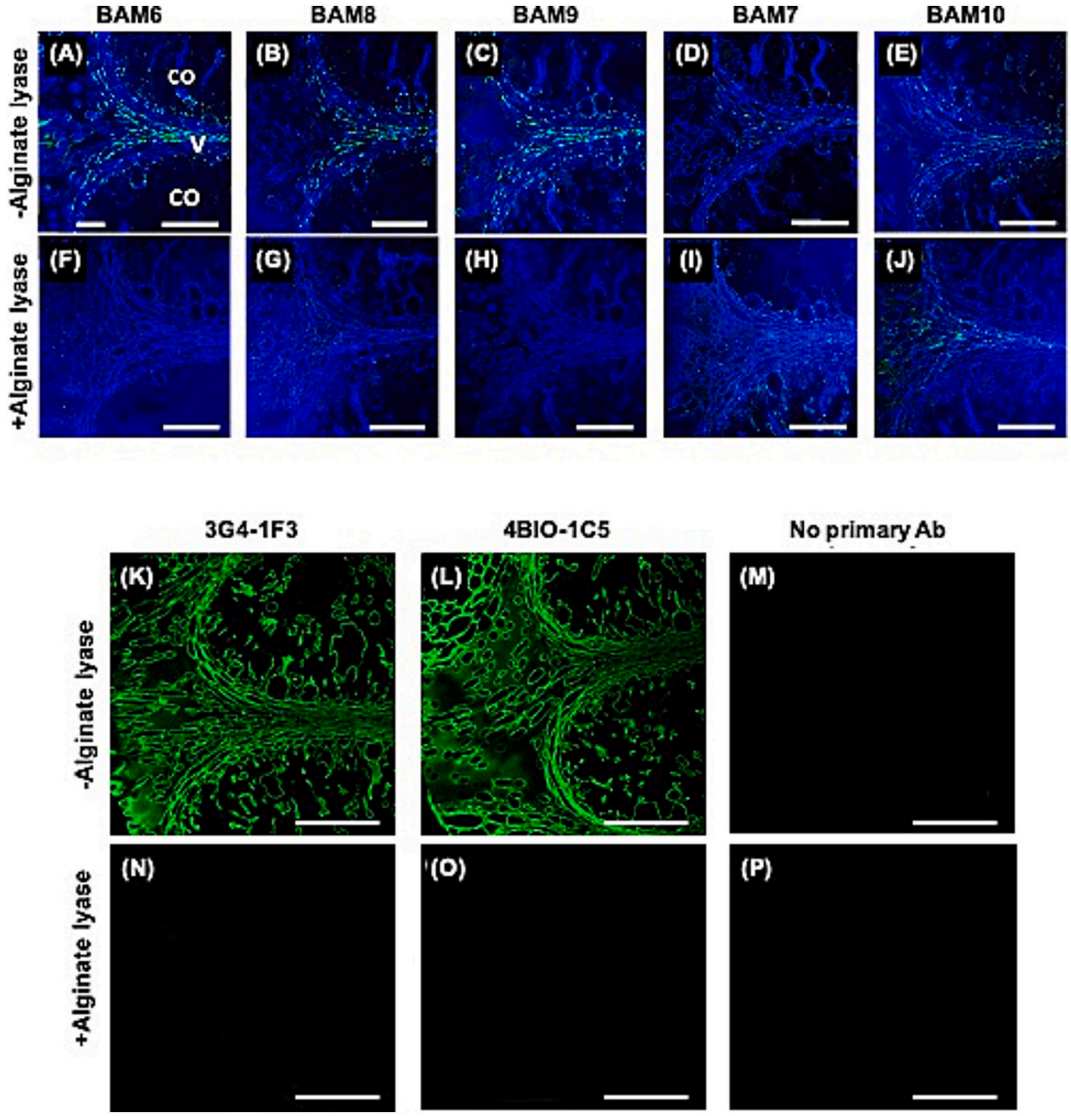

Fig. 2. Immunofluorescence imaging using calcofluor (blue) and anti-alginate BAM mAbs (green) applied to 1 μm resin sections of *Fucus vesiculosus* female receptacles. The images show part of two conceptacles (**co**) separated by vegetative tissue (**v**) as shown in (**A**). Sections (**F**-**J** and **N**—**P**) were pre-treated with alginate lyase from *Sphingomonas* sp. prior to mAb probing. Sections shown in (**K**—**P**) were not counterstained with calcofluor because of the almost complete overlap with 3G4-1F3 and 4BIO-1C5 labelling. Scale bars = 100 μm. (For interpretation of the references to colour in this figure legend, the reader is referred to the web version of this article.)

than for BAM6, BAM8 and BAM9, but also restricted to the septum of tissue between concepticles (Fig. 2D and E). However, whereas BAM6, BAM8 and BAM9 binding was essentially abolished by alginate lyase (Figs. 2F-2H), this was not the case for BAM7 and BAM10, and for BAM10 in particular, significant binding remained after alginate lyase treatment (Fig. 2I and J). For all the BAM mAbs, labelling had a scattered, punctate appearance and appeared to be localised not within cell walls, but rather adhered to the outer surface of walls. Labelling patterns produced with the two commercial mAbs was distinctly different to that of the BAM mAbs. For both 3G4-1F3 and 4BIO-1C5, labelling was present in all cell walls of all tissues within and surrounding female concepticles (Fig. 2K and L). Also, in contrast to the BAM mAbs, the epitopes recognised by 3G4-1F3 and 4BIO-1C5 were restricted to cell walls, rather than on the surface of walls or intercellular spaces (Fig. 2K and L). Binding of 3G4-1F3 and 4BIO-1C5 was abolished by alginate lyase treatment (Fig. 2N and O).

The location of alginate epitopes was analysed at higher magnification with BAM6 and 4BIO-1C5 (Fig. 3). This imaging confirmed that the alginate structures recognised by BAM6 were located on the outer surface of cell walls and often occurred with a punctate distribution (Fig. 3A and C). It also confirmed that the alginate structures recognised by 4BIO-1C5 were located at a position corresponding to cell walls themselves, with labelling across the entire width of walls. This was supported by the fact that 4BIO-1C5 almost exactly coincided with labelling produced by calcofluor, a ß-glucan specific stain that labels cellulose in cell walls (Fig. 3B and D).

3.3. Analysis of seasonal flux of alginate epitopes in wild algal species

Using carbohydrate microarrays, we investigated the relative abundance of alginate epitopes extracted from 17 algal species (**Supplemental Table 3)** collected from the wild on the coast near Roscoff in spring and autumn of 2015–2017. Constituent polysaccharides were sequentially extracted with $CaCl_2$, HCl, Na_2CO_3 and KOH. Extractions were printed as microarrays and probed with 8 alginate-directed mAbs. Mean spot signal intensities from three replicate array experiments are presented as a heatmap in Supplemental Fig. 4.

The signals from the $CaCl_2$ and HCl extracts were uniformly low,

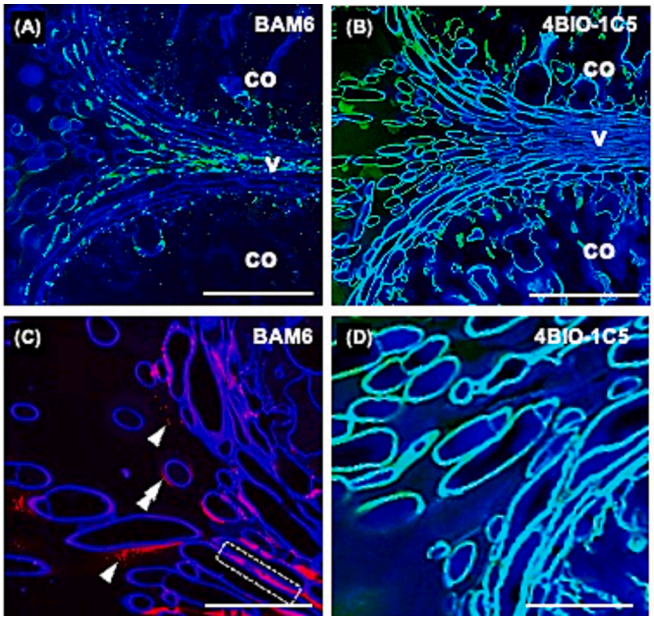

Fig. 3. Immunofluorescence imaging of 1 μm resin sections of *Fucus vesiculosus* female receptacles. Sections were probed with BAM6 (green in **A** and pink in **C**) or 4BIO-1C5 (green in **B** and **D**). All sections were counterstained with calcofluor (blue). Images (**A**) (**B**) show part of two females conceptacles (**co**) separated by vegetative tissue (**v**). Images (**C**) and (**D**) show female conceptacles at higher magnification. Scale bars (**A**) and (**B**) = 100 μm, (**C**) and (**D**) = 50 μm. (For interpretation of the references to colour in this figure legend, the reader is referred to the web version of this article.)

indicating little alginate had been extracted with these solvents. Conversely, signals from both Na_2CO_3 and KOH were relatively high for most species and antibodies. Moreover, the overall binding profiles across species, antibodies and sample times were broadly similar for the Na_2CO_3 and KOH fractions (Supplemental Fig. 4). We were particularly interested to examine seasonal differences (i.e., between the October and April sample sets) and examined the KOH data in more detail. Mean spot signals from KOH samples for April 2016 were subtracted from those of October 2015 and similarly for April 2017 and October 2016. These data are presented in Supplementary Figs. 5 **A** and 5B, respectively.

These analyses revealed notable differences in alginate epitope abundance between species and across seasons and years. For example, comparing October 2015 and April 2016 there was a general trend for most species that signals for mAbs 4B10—1C5 and 3G4-1F3 decreased in the April samples compared to the October samples, whereas signals for most other mAbs increased (Supplementary Fig. 5 **A**). This was the case for *Fucus serratus, Bifurcaria bifurcate, Saccharina latissimi* and *Dictyota dichotoma.* However, for some species including *Laminaria hyperborea*, *Colpomenia peregrina* and *Himanthalia elongata,* all of the alginate epitopes increased in relative abundance in April 2016 compared to October 2015. Conversely, for other species, including *Pelvetia canaliculate*, *Ascophylum nodosum*, *Halidrys siliquosa* and *Dictyopteris polypodioides*, there was a decrease in the relative abundance of all or nearly all alginate epitopes in April 2016 compared to October 2015. A very different profile of epitope abundance was observed for the October 2016/April 2017 sample set (Supplementary Fig. 5B). In this case, the relative abundance of almost all epitopes was decreased in all species sampled in April 2017 compared to October 2016.

4. Discussion

The use of an extensive library of well-defined alginates with known M and G block ratios determined by NMR provided new insights into epitopes recognised by alginate-binding mAbs and placed them into four clear clades. None of the mAbs had a binding preference for alginates containing alternate M and G (i.e., MG and MGM), but they differed in their binding preferences for alginate containing adjacent M or G (i.e. GG, GGG, MM etc). Whilst BAM6, BAM8 and BAM9 all had a binding preference for MM, BAM10 had a binding preference for GG. BAM7 bound to both GG and MM, indicating that for BAM7, the most important factor determining binding is the presence of adjacent identical residues per se, rather than if they contain D-mannuronate or L-guluronate. These findings are in agreement with previous evidence based on ELISAs that BAM6 binds to a mannuronate-rich epitope and that BAM7, BAM8 and BAM9 are closely related and recognise epitopes that can comprise either D-mannuronate or L-guluronate (Thomas et al., 2016). The fact that the epitope recognised by BAM10 appeared to be more resistant to alginate lyase degradation was also in agreement with previous findings, as was the fact that, unique amongst the BAM mAbs, BAM7 also bound to HG-containing pectins (Thomas et al., 2016). Considering the cross reactivity of BAM7, the binding of the anti-HG mAb LM7 to some alginates was not entirety surprising. Presumably, the fact that HG and alginates are both comprised of repeating 1,4-linked uronic acids provides sufficient for them to act as mimotopes of each other for some antibodies.

The specificities of the two commercial mAbs, 3G4-1F3 and 4BIO-1C5 have not previously been reported in detail but our work revealed they both have strong binding preferences for guluronate-rich alginate and are therefore distinct from any of the BAM mAbs. This is significant because, when used in conjunction with the BAM mAbs that recognise mannuronate-rich epitopes (BAM6, BAM8 and BAM9) a set of probes is available that enables us to track the spatiotemporal differential regulation of mannuronate and guluronate. The subcellular scale of this regulation was revealed by the immunofluorescence microscopy which demonstrated that the guluronate-rich epitope recognised by 3G4-1F3 and 4BIO-1C5 was ubiquitous in the *Fucus* sp. tissues analysed and appeared to be present across the entirely of cell walls, whereas the mannuronate-rich epitope recognised by BAM6, BAM8 and BAM9 had a markedly different location on the outer surface of cell walls or between cells. It is reasonable to assume that this tight spatial regulation is driven by the need to match functional requirements at particular cellular locations with the physical and chemical characteristics of alginates that vary according to M and G content and distribution, for example properties of calcium-mediated alginate gels.

The strength per se and rheological properties of alginate gels is highly dependent on G block content (Willats et al., 2001a). Alginates with a higher G content (and longer G blocks) generally form gels that are stronger but more brittle whereas alginates rich in M blocks produce softer and more elastic gels (Willats et al., 2001a). Thus, the concerted activities of mannuronate synthesis and selected conversion of mannuronate to guluronate by mannuronan C5-epimerases provides multiple functionally distinct materials. This strategy is reminiscent of that evolved by land plants based on another uronic acid polymer, homogalacturonan (HG), that forms calcium-mediated gels (Chuhuan et al., 2021). HG is comprised of α-(1–4)-galacturonic acid (GalA) and is initially synthesised and inserted into cell walls in a highly methylesterified form. It may then be de-methylesterified by pectin methyl esterases and the degree and pattern of remaining esters greatly influences HG gelling properties (Chuhuan et al., 2021; Willats et al., 2000; Willats et al., 2001b). In land plants, stronger gels formed by HG with low degrees of methyl esterification are usually located between cells (in middle lamellae) and form a 'glue' that is critical for cell-to-cell adhesion (Chuhuan et al., 2021; Willats et al., 2001b). However, our work suggests that in *Fucus* sp., the guluronate-rich alginate associated with stronger gels (and recognised by 3G4-1F3 and 4BIO-1C5) is located within cell walls, not between them. Moreover, the mannuronate-containing epitope recognised by BAM6, BAM8 BAM9 and likely associated with softer and more elastic gels was localised to the outer surface of cells and between them. The physical, environmental, and

developmental challenges encountered by land plant and algal cells and tissues are very different, so it is not surprising that our findings imply differing utilisations of polymer gels with particular properties. Nevertheless, this work reinforces the notion that convergent evolution has operated in these genetically distinct organisms to produce a common strategy based on uronic acid-rich polymers that can be fine-tuned post-synthesis to meet prevailing functional requirements within subcellular domains.

Our data on the seasonal flux of alginate epitopes revealed differences in alginate epitopes between spring and autumn and between years. Between April and October 2016 there were a wide range of variations across species and mAbs, whereas between April and October 2017 there was a much more consistent response such that most epitopes in most species were reduced in April compared to October. Previous studies have identified seasonal variations in the alginate content and structures of limited numbers of algae (Kelly and Brown, 2000; Kumar and Sahoo, 2017) but there is generally a paucity of knowledge about these effects. Our data indicates substantial temporal variation in alginate epitopes and this presumably reflects physiological responses to prevailing environmental conditions which we currently have very limited understanding of. Nevertheless, considering the ecological significance of macro-algae and the commercial importance of variations in yield and composition of their polysaccharide components, it is an area that deserves further investigation.

Supplementary data to this article can be found online at https://doi.org/10.1016/j.tcsw.2024.100136.

CRediT authorship contribution statement

Catherine T. Jones: Writing – original draft, Validation, Supervision, Software, Project administration, Methodology, Investigation, Formal analysis, Data curation, Conceptualization. **Cassie Bakshani:** Writing – original draft, Validation, Software, Methodology, Investigation, Formal analysis, Data curation. **Ieva Lelenaite:** Writing – review & editing, Validation, Supervision, Project administration, Methodology, Investigation, Data curation. **Jozef Mravec:** Visualization, Resources, Methodology, Investigation, Formal analysis. **Stjepan Krešimir Kračun:** Conceptualization, Data curation, Formal analysis, Investigation, Methodology, Resources. **Jeff Pearson:** Resources, Methodology, Investigation, Formal analysis. **Mathew D. Wilcox:** Resources, Methodology, Investigation, Formal analysis. **Kevin Hardouin:** Resources, Methodology, Investigation, Formal analysis, Data curation, Conceptualization. **Sonia Kridi:** Resources, Methodology, Investigation, Formal analysis, Data curation, Conceptualization. **Cécile Hervé:** Writing – review & editing, Writing – original draft, Resources, Methodology, Investigation, Funding acquisition, Formal analysis, Data curation, Conceptualization. **William G.T. Willats:** Writing – review & editing, Writing – original draft, Validation, Supervision, Software, Resources, Project administration, Methodology, Investigation, Funding acquisition, Formal analysis, Data curation, Conceptualization.

Declaration of competing interest

The authors declare that they have no known competing financial interests of personal relationships that could have appeared to influence the work reported in this paper.

Acknowledgments

We thank the BBSRC for support with funding under the Mid-range equipment for biosciences research: ALERT 2019 programme. Also, the Northern Accelerator Connecting Capability Fund (NA-CCF), BBSRC BiSCoP CTP (Bioscience for Sustainable Consumer Products Collaborative Training Partnership) and Procter & Gamble.

References

Bakshani, C.R., Sangta, J., Sommano, S., Willats, W.G.T., 2023. Microarray polymer profiling (MAPP) for high-throughput glycan analysis. JoVE J. Visualized Exp. 199, e65443. https://doi.org/10.3791/65443.

Bojorges, Hylenne, López-Rubio, Amparo, 2023. María José Fabra, Antonio Martínez-Abad, Estimation of alginate purity and M/G ratio by methanolysis coupled with anion exchange chromatography. Carbohydrate Polymers 321, 121285. https://doi.org/10.1016/j.carbpol.2023.121285 https://doi.org/10.1016/j.carbpol.2023.121285.

Chater, P.I., Wilcox, M.D., Brownlee, I.A., Pearson, J.P., 2015. Alginate as a protease inhibitor in vitro and in a model gut system; selective inhibition of pepsin but not trypsin. Carbohydr. Polym. 131, 142–151. https://doi.org/10.1016/j.carbpol.2015.05.062.

Chuhuan, H., Wei, L., Mata, A., Nishinari, K., Fang, Y., 2021. Ions-induced gelation of alginate: mechanisms and applications. Int. J. Biol. Macromol. 177, 578–588. https://doi.org/10.1016/j.ijbiomac.2021.02.086.

Ertesvåg, H., 2015. Alginate-modifying enzymes: biological roles and biotechnological uses. Front. Microbiol. 6. https://doi.org/10.3389/fmicb.2015.00523.

Fangel, J.U., Sørensen, K.M., Jacobsen, N., Mravec, J., Ahl, L.I., Bakshani, C., Mikkelsen, M.D., Engelsen, S.B., Willats, W., Ulvskov, P., 2024. The legacy of terrestrial plant evolution on cell wall fine structure. Plant Cell Environ. 47 (4), 1238–1254. https://doi.org/10.1111/pce.14785.

Kelly, B.J., Brown, M.T., 2000. Variations in the alginate content and composition of Durvillaea Antarctica and D. Willana from southern New Zealand. J. Appl. Phycol. 12, 317–324. https://doi.org/10.1023/A:1008106723185.

Knox, J.P., 2008. Revealing the structural and functional diversity of plant cell walls. Curr. Opin. Plant Biol. 11 (3), 308–313. https://doi.org/10.1016/j.pbi.2008.03.001.

Kumar, W.S., Sahoo, S.D., 2017. A comprehensive analysis of alginate content and biochemical composition of leftover pulp from brown seaweed sargassum. Algal Res. 23, 233–239 c. https://doi.org/10.1016/j.algal.2017.02.003.

Lee, K.J., Marcus, S.E., Knox, J.P., 2011. Cell wall biology: perspectives from cell wall imaging. Mol. Plant 4 (2), 212–219. https://doi.org/10.1093/mp/ssq075.

Mazéas, L., Yonamine, R., Barbeyron, T., Henrissat, B., Drula, E., Terrapon, N., Nagasato, C., Hervé, C., 2023, January. Assembly and synthesis of the extracellular matrix in brown algae. In: In seminars in cell & developmental biology, 134. Academic Press, pp. 112–124. https://doi.org/10.1016/j.semcdb.2022.03.005.

Rydahl, M.G., Hansen, A.R., Kračun, S.K., Mravec, J., 2018. Report on the current inventory of the toolbox for plant cell wall analysis: proteinaceous and small molecular probes. Front. Plant Sci. 9, 581. https://doi.org/10.3389/fpls.2018.00581.

Skjåk-Bræk, G., Donati, I., Paoletti, S., 2015. Alginate hydrogels: Properties and applications. In: Matricardi, P., Alhaique, F., Coviello, T. (Eds.), Polysaccharide hydrogels: characterization and biomedical applications. Pan Stanford Publishing Pte Ltd, Singapore, pp. 449–498. https://doi.org/10.1201/b19751-15.

Thomas, F., Lundqvist, L.C.E., Jam, M., Jeudy, A., Barbeyron, T., Sandström, C., Michel, G., Czjzek, M., 2013. Comparative characterization of two marine alginate Lyases from Zobellia galactanivorans reveals distinct modes of action and exquisite adaptation to their natural substrate. J. Biol. Chem. 288 (32), 23021–23037. https://doi.org/10.1074/jbc.M113.467217.

Thomas, A.T., Amandine, S., Marcus, S.E., Jam2, M., le Moigne, M.-A., Duffieux, D., Knox, J.P., Hervé, C., 2016. Dynamics of cell wall assembly during early embryogenesis in the brown alga fucus. J. Exp. Bot. 67 (21), 6089–6100. https://doi.org/10.1093/jxb/erw369.

Willats, W.G., Limberg, G., Buchholt, H.C., van Alebeek, G.J., Benen, J., Christensen, T. M., Visser, L., Voragen, A., Mikkelsen, J.D., Knox, J.P., 2000. Analysis of pectic epitopes recognised by hybridoma and phage display monoclonal antibodies using defined oligosaccharides, polysaccharides, and enzymatic degradation. Carbohydr. Res. 327 (3), 309–320. https://doi.org/10.1016/S0008-6215(00)00039-2.

Willats, W.G.T., Orfila, C., Limberb, G., Buchholt, H.C., van Alebeek, G.J.W., Voragen, A. G.J., Marcus, S.E., Christensen, T.M.I.E., Mikkelsen, J.D., Murray, B.S., Knox, J.P., 2001a. Pectic homogalacturonan in plant cell walls: implications for pectin methyl esterase action, matrix properties and cell adhesion. J. Biol. Chem. 276 (22), 19404–19413. https://doi.org/10.1074/jbc.M011242200.

Willats, W.G.T., Orfila, C., Limberg, G., Buchholt, H.C., van Alebeek, G.J.W., Voragen, A. G., Marcus, S.E., Christensen, T.M.I.E., Mikkelsen, J.D., Murray, B.S., Knox, J.P., 2001b. Modulation of the degree and pattern of methyl-esterification of pectic homogalacturonan in plant cell walls. Implications for pectin methyl esterase action, matrix properties, and cell adhesion. J. Biol. Chem. 276 (22), 19404–19413. https://doi.org/10.1074/jbc.M011242200.